APPLIED SCIENCES AND ENGINEERING

Orally administered saccharide-sequestering nanocomplex to manage carbohydrate metabolism disorders

Xin Zhao[1], Huijun Zhang[1], Jiacheng Li[1], Meng Tian[1], Juanjuan Yang[1], Songxuan Sun[1], Qixin Hu[1], Liu Yang[2], Shiyi Zhang[1]*

Excessive carbohydrate intake is linked to the growing prevalence of diabetes, nonalcoholic fatty liver disease (NAFLD), and obesity. α-Glucosidases inhibitor, the only Food and Drug Administration–approved drug for limiting the absorption of polysaccharides and disaccharides, is ineffective for monosaccharides. Here, we develop a boronic acid–containing polymer nanocomplex (Nano-Poly-BA), absorbing all saccharides into nanocomplex with the diol/boronic acid molar ratio far above 1, to prevent saccharides' absorption in the gut. The orally administered Nano-Poly-BA is nonabsorbable and nontoxic. When tested against four kinds of carbohydrates and three real-world foods (coke, blueberry jam, and porridge), Nano-Poly-BA shows remarkable after-meal blood glucose reductions in wild-type, type 1, and type 2 diabetic mouse models. In a NAFLD mouse model induced by fructose, Nano-Poly-BA shows substantial reduction of hepatic lipogenesis. In short, the orally administered saccharide-sequestering polymer nanocomplex may help prediabetic, diabetic, overweight, and even healthy people to manage sugar intake.

INTRODUCTION

Overnutrition has been a growing global health threat (*1*, *2*). Excessive sugar intake increases the disease burden of cardiovascular disease (*3*), diabetes (*4*), obesity (*5*), nonalcoholic fatty liver disease (NAFLD) (*6*), and other metabolic disorders (*7*). Policy-making and patient education on sugar restriction have only limited effect, while technical breakthroughs in medication await (*8*). As the only Food and Drug Administration (FDA)–approved medication for limiting sugar intake, the α-glucosidase inhibitor (*9*) (mainly acarbose) is ineffective to monosaccharides (e.g., glucose and fructose), which limits its clinical usage for people adhering to the Western diet (*10*). Beyond diabetes, excessive consumption of fructose has a tight association with NAFLD, nonalcoholic steatohepatitis (NASH), and many other diseases (*6*). However, there is no drug approved or in clinical studies that act to limit the fructose intake.

The gastrointestinal (GI) tract has attracted increasing attention as a therapeutically target for its crucial role in metabolic disorders (*11*, *12*). For sugar intake, the GI tract is the major place where polysaccharides and disaccharides are digested into monosaccharides through enzymolysis and where monosaccharides are transported from the intestinal lumen, across the epithelium, and then into blood (*13*). With respect to these physiological facts, we design polymers appending saccharide-binding units to bind polysaccharides, disaccharides, and monosaccharides in the lower GI tract environment (pH > 6.8), therefore preventing their enzymolysis and absorption and then allowing egestion of undigested saccharides from the body as feces. Boronic acid binds diol on different kind of saccharides (*14*). With the fear of serious side effects caused by the uncontrolled and unwanted interactions between boronic acid and natural glycan units in the blood, biomedical applications of boronic acid–containing polymers were mostly limited to sugar sensing and sugar-responsive delivery of therapeutic agents (*15*–*19*). Contrary to the popular belief, the orally administered synthetic polymers, as therapeutic agents, were approved by FDA with different safety requirements than intravenously administered drugs or implants because they were nonabsorbed in the GI tract and had zero systemic exposure (examples of reasonable abbreviation of safety study in the official pharmacology review of FDA-approved polymer drugs as shown in fig. S21) (*20*). From the safety standing point, the high molar mass (>3000 Da) of these polymer drugs ensures the nonabsorbed property and minimizes systemic side effects. For example, polyethylene glycol (PEG; 3350 Da) is approved as laxative (*21*), polyallylamine (Colesevelam) is a bile acid sequestrant for hyperlipidemia (*22*), polyfluoroacrylic acid (Veltassa) is a potassium sequestrant for hyperkalemia (*23*), and a deprotonated amine-containing polymer (TRC101, recently completed two phase III studies) as a proton sequestrant for metabolic acidosis (*24*). The now available polymer sequestrants are all based on the electrostatic interaction between ion pairs; therefore, 1 M polymer ion is needed to remove just 1 M unwanted ion. With the dynamic exchangeable function of boronic acid–diol binding and the encapsulation property of self-assembled nanostructure, we envisage that the boronic acid–containing polymer nanocomplex (Nano-Poly-BA) could provide a platform for binding saccharide with the diol/boronic acid molar ratio above 1, thereby enabling a safe and effective saccharide binder to prevent their digestion and absorption.

Here, we report the first example of an orally administered polymer nanocomplex (Nano-Poly-BA) for preventing saccharide absorption in the GI tract by serving as a dynamic covalent nano-sequestrant for all types of saccharides (Fig. 1) with the diol/boronic acid molar ratio far above 1. Although there have been extensive studies using boronic acid–containing polymers for diagnosis or responsive delivery of therapeutic cargos for diabetes (*15*–*19*), the application of boronic acid itself as the therapeutic agent is seldom reported (*25*). This manuscript presents a novel utilization of the boronic

[1]School of Biomedical Engineering, Shanghai Jiao Tong University, Shanghai 200240, P. R. China. [2]Shanghai Diabetes Institute, Department of Endocrinology and Metabolism, Shanghai Jiao Tong University Affiliated Sixth People's Hospital, Shanghai Jiao Tong University School of Medicine, Shanghai 200032, China.
*Corresponding author. Email: zhangshiyi@sjtu.edu.cn

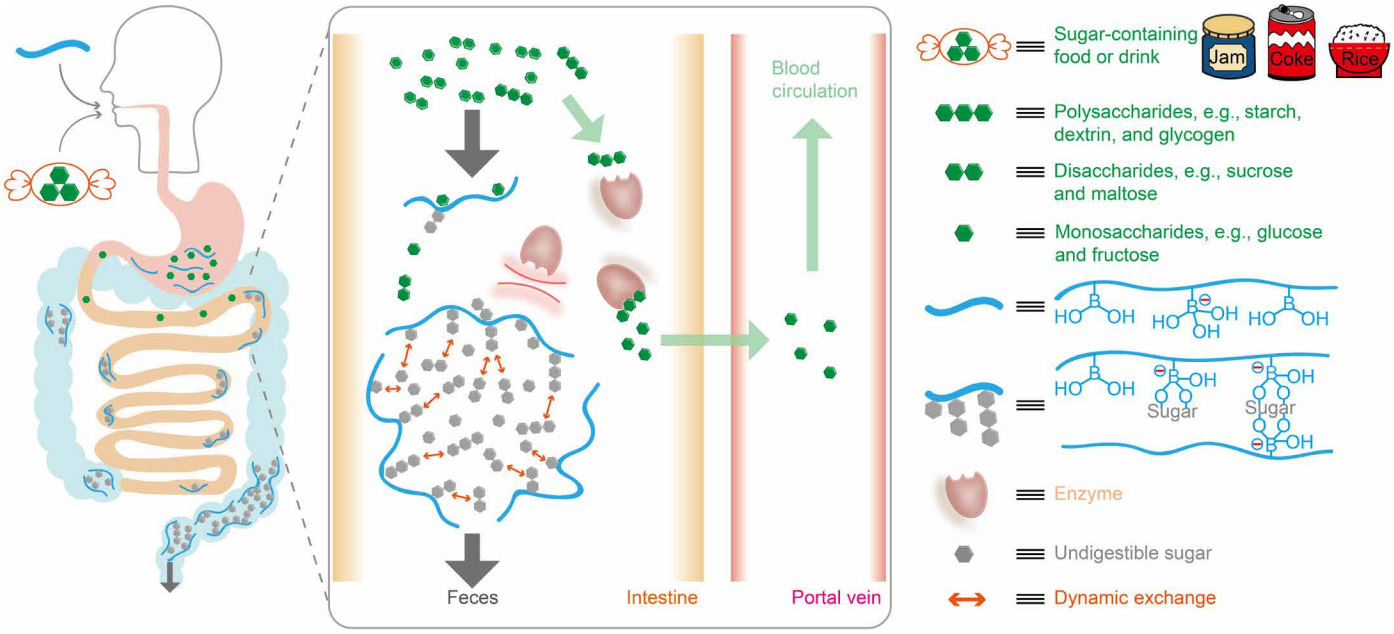

Fig. 1. Schematic illustration of nonabsorbed boronic acid–containing polymer nanocomplex (Nano-Poly-BA) sequestering a full spectrum of saccharides in the lower GI tract, thereby reducing their digestion and absorption by forming the nanocomplex through the dynamic exchangeable bonds between boronic acid groups and diol units.

acid–containing nanoparticle itself as a safe therapeutic agent for the management of multiple disorders of carbohydrate metabolism. Negative charge and/or PEG unit on Poly-BA render nonabsorbed and nonfouling properties, thereby providing a zero systemic exposure and an ideal safety profile. Poly-BA self-assembles into nanostructures in water and serves as the sponge to absorb a large number of saccharides through dynamic bonds. The hierarchical design from molecular level to nano level is highly customizable, owing to the enriched monomer library and one-pot polymer chemistry, and may lead to extensive applications by controlling the absorption of the widely existing saccharide analogs as nutrients, drugs, toxins, and even glycosylated biomolecules for other medical needs.

RESULTS

Boronic acid–containing polymer with optimal saccharide sequestration capability and nonfouling property

We synthesized a library of boronic acid–containing copolymers and studied the structure-property relationship to screen for the optimal saccharide sequestration capability and nonfouling property. The saccharide-sequestering copolymer, Poly-BA, was synthesized from two or three kinds of monomers. The water insoluble 4-vinylphenylboronic acid (4-VPBA) was used as the primary monomer as the saccharide-binding unit (*19*). Eight different acrylic monomers, M1 to M8, charged or neutral, negatively charged or positively charged, hydrophilic or hydrophobic, were used as comonomers (Fig. 2A and table S1). 4-VPBA was copolymerized with comonomers (M1 to M8) with the mass ratio of 1/1 by microemulsion polymerization and purified to yield boronic acid–containing copolymers P1 to P8, respectively. Anti-enzymolysis test was conducted to evaluate Poly-BA's effectiveness in sequestering different saccharides from enzymolysis. In principle, polysaccharides and disaccharides need to be hydrolyzed by enzymes into monosaccharides for absorption. Poly-BA and disaccharides/polysaccharides could form some kind of complex to limit the accessibility of necessary enzymes to disaccharides or polysaccharides, thereby making a portion of disaccharides/polysaccharides undigestible (Fig. 2I). Forty percent of a disaccharide (maltose) could be hydrolyzed by the corresponding enzyme with P1 to P8 (Fig. 2B), while less than 60% of a polysaccharide (glycogen) could be hydrolyzed with P1 to P8 (Fig. 2C). Different comonomers had different contributions to the saccharide-sequestering capability (Fig. 2, B and C, and fig. S4). M1- and M4-derived P1 and P4 had the best saccharide sequestration capability among all eight copolymers for five common dietary saccharides. Higher water solubility of P1 and P4 and resulting better accessibility of boronic acid groups may explain their superior saccharide-sequestering capability (table S1).

For our purpose of fast transition through GI tract, the fouling of Poly-BA on mucus should be avoided. Thus, we studied the nonfouling property of Poly-BAs on mucus, a highly glycosylated network (*26*). Poly-BAs were labeled with fluorescein by adding fluorescent comonomer during the polymerization (table S1). Then, we conducted an ex vivo mucus retention test by washing fresh porcine duodenum after the addition of fluorescent-labeled Poly-BA. As shown in Fig. 2, D and E, negatively charged P1 was easily washed out by phosphate-buffered saline (PBS) with seldom retention (1%), while positively charged P4 was mostly retained (66%). Neutral hydrophilic P5 showed less retention (18%) than that of neutral hydrophobic P8 (33%). The mucus network is hydrophobic and negatively charged (*26*). Therefore, hydrophobic and positively charged polymers are intrinsically mucus adhesive, while hydrophilic and negatively charged polymers are more likely to be nonfouling (*26*). Considering the excellent biocompatibility of pegylated polymer, we further synthesized terpolymer with 4-VPBA, M1, and M5 to obtain P19 to P21 (table S1). Balancing the excellent

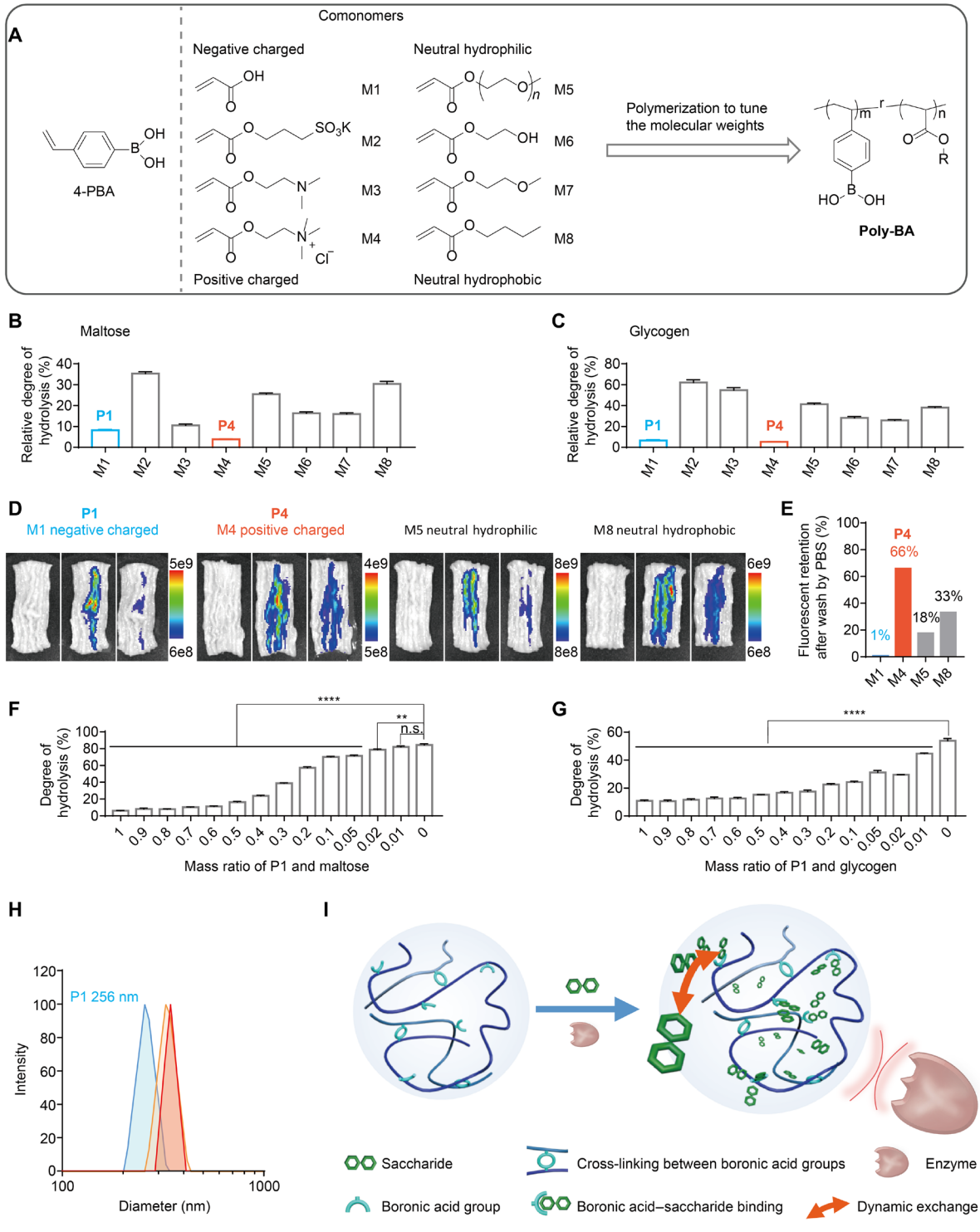

Fig. 2. Study of structure-property relationship of a library of the boronic acid–containing polymers for optimal saccharide binding capability and nonfouling property. (**A**) A library of different Poly-BAs was obtained from the copolymerization of 4-vinyl phenylboronic acid (4-VPBA) with eight different comonomers. (**B** and **C**) In enzymolysis tests, M1 and M4 contributed significantly to reducing the degree of hydrolysis of disaccharides (B) and polysaccharides (C) by enzymes. $n = 4$. (**D** and **E**) Nonfouling tests of fluorescein-labeled Poly-BAs on the mucus of porcine duodenum showed that the negatively charged P1 was completely washed out by PBS with seldom retention, while the positively charged P4 was mostly retained on the mucus. Left: original duodenum; middle: after adding Poly-BA; right: after washing. (**F** and **G**) Enzymolysis tests with different mass ratio of P1 and saccharide showed that P1 had capability of binding more than 1 M equivalent disaccharides (F) and polysaccharides (G) to prevent their hydrolysis by enzymes. One-way ANOVA with $^{**}P \leq 0.01$ and $^{****}P \leq 0.0001$; $n = 3$. n.s., not significant. (**H**) DLS results showed that P1 formed nano-complex in SIF, and it swelled after binding saccharides. (**I**) Schematic illustration of Nano-Poly-BA binding to polysaccharides and disaccharides through dynamic interaction, therefore preventing their enzymolysis by more than 1 M equivalent ratio. Error bars show SEM.

saccharide-sequestering capability and nonfouling property, P1 and P20 (fig. S10) were selected for further study.

We explored Poly-BA's saccharide-sequestering capacity and studied its nanostructures in water. We conducted a series of anti-enzymolysis tests with different mass ratio of P1 to saccharide from 0.01 to 1 (0.012 to 1.2 as molar ratio of boronic acid group to diol unit). As shown in Fig. 2F, 1/50 of P1 was able to significantly reduce the hydrolysis of maltose by enzyme, and 1/2 of P1 could reduce enzymolysis to below 20%. For glycogen, a polysaccharide, even 1/100 of P1 suppressed the hydrolysis of glycogen significantly (Fig. 2G). These results showed that one equivalent of boronic acid group on P1 could reduce the hydrolysis of more than one equivalent of saccharides. The high saccharide-sequestering capacity of P1 also recurred in sucrose, starch, and dextrin (fig. S6). By changing the BA ratio of P1 to higher or lower degrees, we found that the saccharide-sequestering capability was disproportionate with the BA ratio (fig. S7), implying that the interaction between saccharide and Poly-BA was not merely the dynamic covalent binding between boronic acid and diol. We hypothesized that the super saccharide-sequestering capability of P1 partially came from the unique self-assembled nanostructure. As shown in Fig. 2H, dynamic light scattering (DLS) results showed that P1 formed nanocomplex with the average hydrodynamic diameter of 256 nm in simulated intestinal fluid (SIF), while the average diameter increased notably with the addition of sucrose or maltose. Transmission electron microscopy (TEM) imaging also confirmed the nanocomplex structure of P1 with the diameter around 250 nm (fig. S8, A and D). After adding sucrose or maltose, P1/saccharide nanocomplex showed expanded morphology (fig. S8, B, C, E, and F). Results of DLS and TEM indicated that P1 nanocomplex could expand its volume after encapsulating saccharides. Nuclear magnetic resonance diffusion-ordered spectroscopy measurement of sucrose with or without P1 in deuterated SIF demonstrated that sucrose had lowered diffusion rate with P1 (fig. S9), confirming that sucrose was interacting with P1 by the dynamic exchangeable binding between boronic acid and diol. The dynamic exchangeability allowed one equivalent boronic acid unit to interact with multiple equivalents of saccharides, which have been absorbed in the nanocomplex. In short, Poly-BA first self-assembled into a nanocomplex, and then, this nanocomplex absorbed saccharides by dynamic exchangeable bond between diol and boronic acid. In the nanocomplex, not every saccharide molecule has the direct interaction with boronic acid group at the one moment. Still, the movement and diffusion of saccharides were notably limited because of the dynamic exchangeable binding and the hierarchical nanostructure; therefore, Nano-Poly-BA (Poly-BA with nanocomplex structure) could trap more than one equivalent of saccharides and then prevent them from hydrolysis by corresponding enzymes (Fig. 2I).

Saccharides retention in simulated GI environments

To reveal the Nano-Poly-BA's saccharide-sequestering capability for broader saccharide spectrum in complicated GI environments, we designed and conducted three in vitro experiments with P1 and P20 (Fig. 3A). First, for disaccharides (sucrose in Fig. 3B and maltose in fig. S11A) and polysaccharides (dextrin in Fig. 3C, starch in fig. S11B, and glycogen in fig. S11C), less than 10% of saccharide could be hydrolyzed by enzymes in the presence of Nano-Poly-BA in SIF. Second, monosaccharides needed to diffuse freely to the corresponding transporters on absorptive cells for absorption. Nano-Poly-BA could interact with monosaccharides and prevent their free diffusion, in turn, limiting their absorption. To study this process, we used a dialysis bag to mimic the intestinal membrane, which was permeable to glucose, but not to the polymer, and mixed glucose with P1 in SIF (Fig. 3D). The glucose concentration outside of the dialysis bag was measured as an indicator for Nano-Poly-BA's glucose-binding capacity. Figure 3 (E and F) shows that the diffusion rate of glucose greatly slowed down, and about half of glucose was still trapped in the dialysis bag after 6 hours compared with the control experiment. Incubation in simulated gastric fluid and then redissolving in SIF simulated the procedure of Nano-Poly-BA passing through the stomach environment to duodenum, and we found that the pH change did not affect the saccharide-sequestering capacity of Nano-Poly-BA (fig. S12). By adding nonsaccharide nutrient model molecules into the mixture of P1, maltose, and α-glucosidase, we further found that the Nano-Poly-BA–induced reduction of hydrolysis of saccharide by enzyme was barely affected by lipid, protein, and vitamin (fig. S19), owing to the lack of formation of chemical binding (fig. S20). To summarize the in vitro experiments, after passing through acidic stomach to small intestinal environment, Nano-Poly-BA could specifically bind all types of saccharides and prevent their hydrolysis or absorption efficiently while being inert to other nutrients that are encouraging for further studies in vivo.

Nano-poly-BA is nonfouling, nonabsorbed, and safe

We conducted a set of experiments to study the nonfouling and nonabsorbed properties of Nano-Poly-BA. To confirm the nonfouling nature, an ex vivo mucus retention test was conducted. As shown in fig. S14, sulfo-Cy5–labeled Nano-Poly-BA (fig. S13) could be easily washed out and was seldom retained on the surface of fresh porcine duodenum, revealing that the nonfouling Nano-Poly-BA had minimal interaction with the mucus surface (Fig. 3J). To study the nonabsorbed property, we conducted biodistribution experiments in mice. Mice were kept fasting to exclude the impact of uncontrolled food intake. As shown in Fig. 3G, 15 min, 60 min, 2 hours, and 5 hours after the gavage of sulfo-Cy5–labeled Nano-Poly-BA, fluorescent emission was only observed in the abdominal area without diffusion and then completely disappeared after 24 hours. Next, selected critical organs were isolated after the gavage, and no fluorescent signal was able to be detected, which implied that Nano-Poly-BA had the zero systemic exposure (Fig. 3H). We further studied the passage of Nano-Poly-BA through GI tract, by ex vivo imaging the whole GI tract at different time points after the gavage (Fig. 3I). As short as 15 min, a portion of polymer reached as far as approximately one-third of the length of small intestine, manifesting the fast evacuation of P1 from stomach to intestine. Between 1 and 3 hours, the fluorescence signal was spread out the whole GI tract, and green feces excreted by the mice were observed after 1 hour (fig. S15A). No fluorescence was detectable after 24 hours, indicating the rapid passage of Nano-Poly-BA. We also evaluated the GI transit with the impact of uncontrolled food intake, by permitting the mice to free access to standard chow and water after gavage of sulfo-Cy5–labeled Nano-Poly-BA (fig. S16). Fluorescent polymer rapidly passed to lower GI tract and was completely eliminated within 75 min, implying strong binding of Nano-Poly-BA with food allowing faster passage. These results collectively demonstrated that Nano-Poly-BA was nonfouling and nonabsorbed in GI tract (Fig. 3J).

Because of the zero systemic exposure, minimal interaction with GI surface, and fast passage, our acute toxicity study has proven an acceptable safety profile of Nano-Poly-BA. No adverse effect was

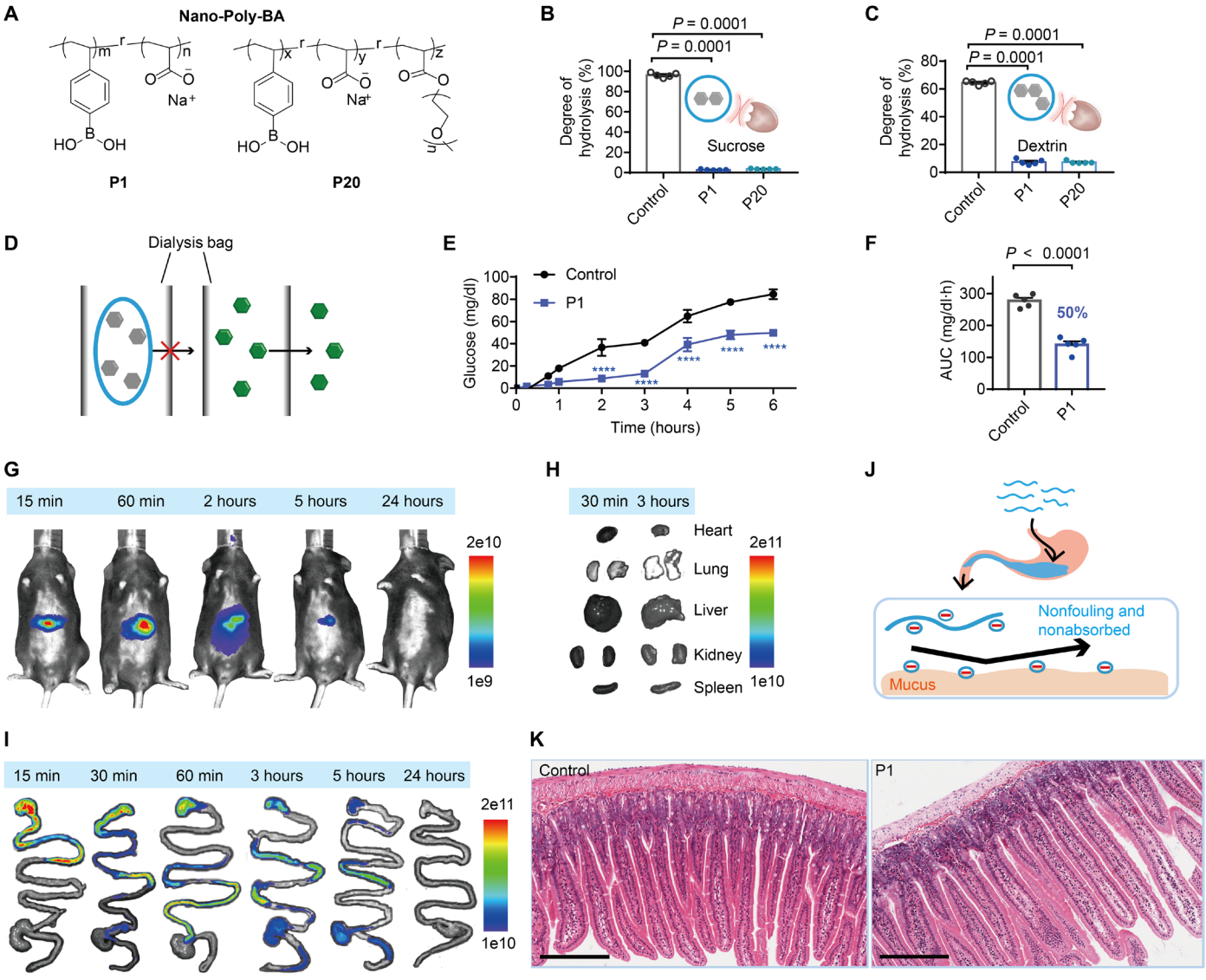

Fig. 3. In vitro assessment of Nano-Poly-BAs in the prevention of saccharides digestion and glucose absorption in the simulated intestinal environment, biodistribution, and acute toxicity studies in mice. (**A**) Chemical structures of selected Nano-Poly-BAs (P1 and P20). (**B** and **C**) Results of enzymolysis tests showed that P1 and P20 greatly reduced the degree of hydrolysis of disaccharides and polysaccharides by enzymes. One-way ANOVA, $n = 5$. (**D**) Schematic illustration of Nano-Poly-BA binding to monosaccharide, therefore limiting its diffusion. (**E**) Results of the glucose diffusion test indicated that Nano-Poly-BAs retained the glucose and prevented its free diffusion. Two-way ANOVA with $^{****}P \leq 0.0001$, $n = 5$. (**F**) The area under the curve (AUC) results of (D). Student *t* test, two-tailed, $n = 5$. (**G**) The whole-body in vivo fluorescence imaging 15 min, 60 min, 2 hours, 5 hours, and 24 hours after gavage of sulfo-Cy5 labeled Nano-Poly-BA. (**H**) Ex vivo imaging of five critical organs 30 min and 3 hours after gavage. No fluorescence signal was detected in those critical organs. (**I**) Ex vivo imaging of the whole GI tract harvested from stomach to large intestine, 15 min, 30 min, 60 min, 3 hours, 5 hours, and 24 hours after gavage, showed a gradual transition of sulfo-Cy5 labeled Nano-Poly-BA from stomach to large intestine without any detectable retention. (**J**) Schematic illustration of the nonfouling and nonabsorbed properties of Nano-Poly-BA in the GI tract. (**K**) Representative histology images of proximal intestine (duodenum) of mice, which were set to free drinking of either normal sterile water or P1 solution (5 wt %) for 7 days, showed no physiological differences between two groups. Scale bars, 200 μm. Error bars show SEM.

observed, at a high-dose oral administration (5 g/kg per day) of Nano-Poly-BA on C57BL/6J mice for continuous 7 days. The body weights among P1, P20, and saline control groups showed the same trend, with no detectable differences (fig. S15B). Histology images of the proximal intestine (duodenum), harvested after 1-week free drinking of P1 [5 weight % (wt %)], showed healthy epithelium structures and no pathological difference with water group (Fig. 3K), implying the lack of local impact of Nano-Poly-BA on GI tract. These results demonstrated that Nano-Poly-BA was nontoxic in the high dose (5 g/kg per day).

Nano-Poly-BA reduces postprandial glucose

In the initial in vivo test, we conducted a standard oral glucose tolerance test (OGTT) and oral carbohydrates tolerance tests (OCTTs) in wild-type mice to assess whether Nano-Poly-BA could act as a full-spectrum saccharide binder (Fig. 4A). We challenged mice with

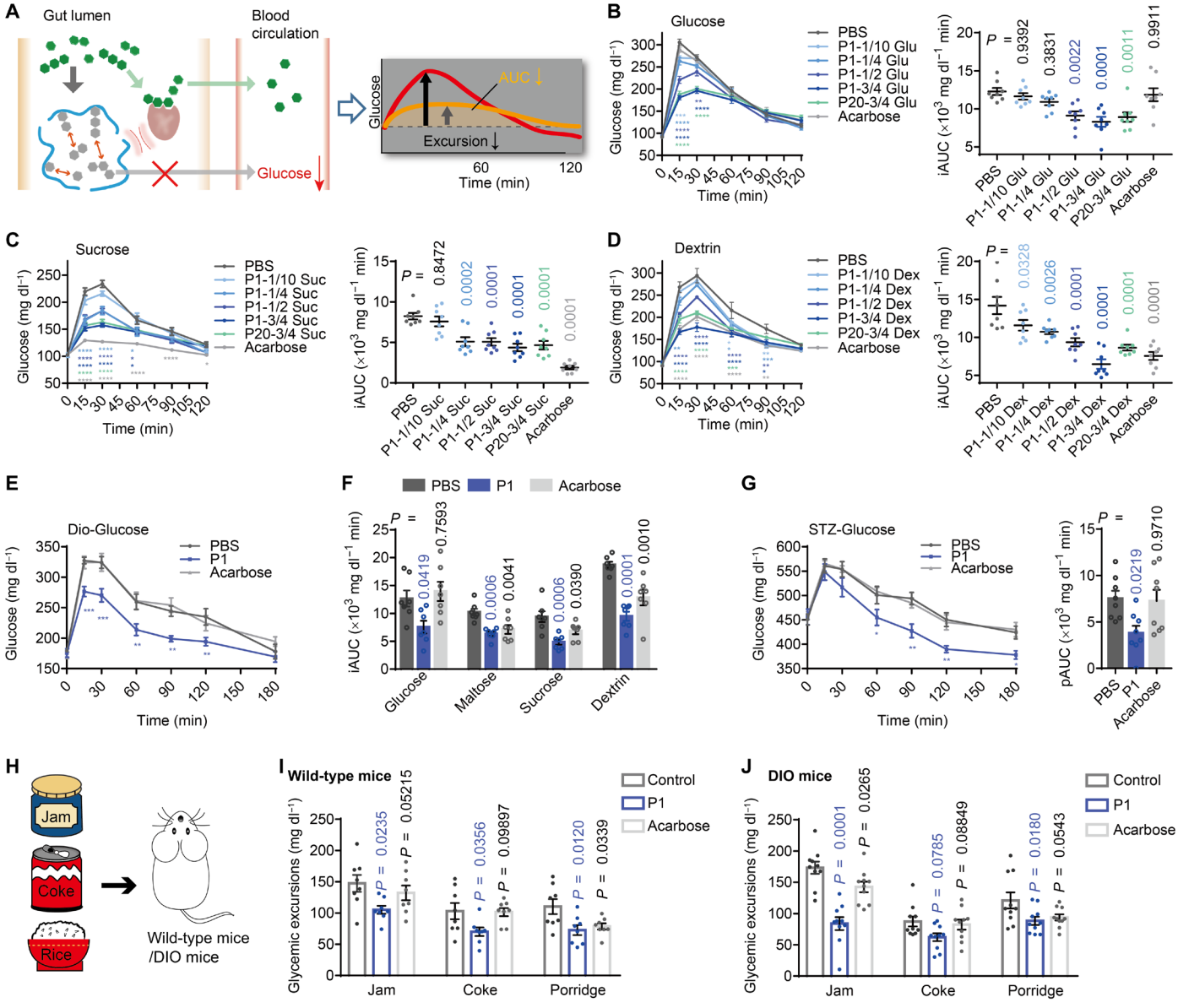

Fig. 4. Blood glucose lowering effect in wild-type, type 1 diabetic, and type 2 diabetic mice with saccharides and real-world foods. (**A**) The representative illustration shows that Nano-Poly-BA binds saccharides in gut lumen and reduces glucose intake, thereby suppressing the PPG excursion. OCTT curves and incremental area under the curves (iAUC) of wild-type mice gavaged with different saccharides [(**B**) a monosaccharide, glucose; (**C**) a disaccharide, sucrose; (**D**) a polysaccharide, dextrin] and Nano-Poly-BAs (P1 and P20) showed dose-dependent reduction of PPG by Nano-Poly-BA binding to saccharides. Mice gavaged with PBS were used as a negative control and acarbose as a positive control. Nano-Poly-BA has glucose lowering effect for monosaccharides, disaccharides, and polysaccharides. Two-way ANOVA, $n = 8$ for blood glucose curves; one-way ANOVA, $n = 8$ for iAUC. (**E**) Blood glucose curves of an OGTT conducted on diet-induced obesity (DIO) mice gavaged with glucose and P1 (PBS and acarbose as controls). Two-way ANOVA, $n = 7$. (**F**) iAUC results of DIO mice, gavaged with different kind of saccharide and P1 (PBS and acarbose as controls). One-way ANOVA, $n = 7$. (**G**) Blood glucose curves and positive incremental area under the curves (pAUC) results of an OGTT of streptozotocin (STZ)–induced type 1 diabetic mouse model, gavaged with glucose. Two-way ANOVA, $n = 8$. (**H**) Schematic illustrating that lean mice and obese mice were challenged with PBS (control), blueberry jam, coke, or rice porridge. (**I**) Glycemic excursions of OCTT results for lean mice ($n = 8$), and (**J**) glycemic excursions of OCTT results for obese mice ($n = 10$), indicating the well control of after-meal glucose for real-world foods. One-way ANOVA for (I) and (J). $^{*}P \le 0.05$, $^{**}P \le 0.01$, $^{***}P \le 0.001$, and $^{****}P \le 0.0001$ for (B) to (E) and (G). Error bars show SEM.

monosaccharide (glucose), disaccharides (sucrose and maltose), and polysaccharide (dextrin) after gavage of PBS, P1, P20, and acarbose. In PBS control group, a significant rise of blood glucose level was detected 15 min after the saccharides load, and a hill-like curve was depicted in a 2-hour period [black line in Fig. 4 (B to D and fig. S18]. Acarbose, an FDA-approved drug that inhibits enzymes needed to hydrolyze oligosaccharides and disaccharides into glucose and other monosaccharides, was chosen to make the head-to-head comparison. Although acarbose effectively lowered postprandial glucose (PPG) in polysaccharide and disaccharide groups (Fig. 4, C and D, and fig. S18), it did not work for glucose (Fig. 4B). In a sharp contrast, P1 and P20 efficiently reduced the glucose excursions (GEs; the

increased glucose level from the glucose level at t = 0 min to the peak glucose value of PPG, 51.5 ± 14.5% and 48.3 ± 13.6% reduction, respectively) and incremental area under the curves (iAUC; 32.5 ± 6.0% and 27.5 ± 5.5% reduction, respectively) when the dose of Nano-Poly-BA was ¾ the dose of glucose for the glucose challenge. These results indicated that Nano-Poly-BA suppressed PPG excursion after oral glucose load. In OCTT experiments, Nano-Poly-BA had similar PPG control effectiveness as acarbose for disaccharides and polysaccharide [¾ the dose of saccharide in Fig. 4 (C to D) and fig. S18]. Furthermore, P1 nanocomplex showed dose-dependent reduction of PPG after saccharide challenge. For monosaccharide (glucose), oral administration of P1 nanocomplex in ½ the dose of glucose was able to bring significant reduction in iAUC (Fig. 4B). For disaccharides (sucrose and maltose), P1 nanocomplex could lower iAUC significantly in ¼ the dose of disaccharides (Fig. 4C and fig. S18). For polysaccharide (dextrin), even 1/10 the dose of polysaccharide loading of P1 nanocomplex reduced iAUC effectively (Fig. 4D). These results indicated that a small amount of P1 nanocomplex could suppress after-meal blood glucose effectively. All these results demonstrated that P1 nanocomplex is an ideal full-spectrum saccharide binder for further evaluations.

In addition, to test our hypothesis that P1 nanocomplex acts as a saccharide binder locally in the GI tract and not through a systemic effect, we compared the impact of oral P1 treatment on an OGTT versus an intraperitoneal glucose tolerance test (IPGTT). The OGTT study evaluated P1's impact on glucose absorption, while an IPGTT skipped the step of intestinal absorption excluding the polymer-glucose interaction in the GI tract and tested for other systemic effects. As shown in fig. S17, plasma GE reduced significantly in OGTT, whereas iAUC was reduced by 36.2 ± 13.7%. In contrast, P1 had no positive impact on IPGTT, which suggested that P1 bounds to saccharides locally in the GI tract and not by a systemic effect.

We further studied Nano-Poly-BA in diabetic mouse models. In Fig. 4E, diet-induced obesity (DIO) mice, a type 2 diabetic mouse model (*27*), showed significant raise of glucose levels (150.8 ± 15.3 mg dl^{-1}) after glucose administration (0.5 g/kg). P1 nanocomplex reduced the glucose levels at all time points within 3 hours. P1 nanocomplex showed remarkable reduction of glucose response in iAUC results for a full spectrum of saccharides (32.7 to 41.2% reduction in iAUC), which outperformed acarbose for all the saccharides tested (Fig. 4F). In a streptozotocin (STZ)–induced type 1 diabetic mouse model (Fig. 4G), P1 nanocomplex substantially shortened the time for the glucose level restoring to the baseline level (60 min for P1 and 120 min for PBS and acarbose) and significantly reduced the positive incremental area under the curves (pAUC) of OGTT (44.8 ± 40.6% reduction). These results collectively demonstrated that P1 nanocomplex could effectively reduce after-meal glucose levels in both type 1 and type 2 diabetic mouse models for a full spectrum of saccharides.

Furthermore, we studied Nano-Poly-BA for real-world foods and drinks. We selected high-carbohydrate blueberry jam, cola, and porridge, because of their popularity in either Western or Eastern menu and their potential risk to diabetic and prediabetic populations. In lean mice (Fig. 4, H and I), P1 nanocomplex significantly protected mice from fast postmeal GE in all tested foods (28.7 to 34.1% reduction in GE). On the contrary, acarbose did not work for jam or coke, whose major component is monosaccharide. The performance of P1 nanocomplex on DIO mice (Fig. 4J; 26.0 to 49.6% reduction in GE) mirrored the results found on wild-type mice, suggesting the robust efficacy of P1 nanocomplex on lowering PPG for both lean and obese mice. Thus, in addition to refined carbohydrates, Nano-Poly-BA can manage sugar intake and control blood glucose level for real-world foods and drinks, which may have great clinical significance for a wide population.

Nano-Poly-BA reduces fructose absorption and liver adiposis

The association of excess ingestion of fructose with the increasing risks of hyperfructosemia, fructosuria, obesity, hypertension, NAFLD, and NASH is mediated by stimulating de novo lipogenesis and blocking fatty acid oxidation in the liver (*6*). Sadly, fructose, as the predominant sweetening agent added in modern foods and drinks either as sucrose (50% fructose) or as high-fructose corn syrup (42 or 55% fructose), is heavily consumed. However, no drugs are available to prevent the absorption of fructose. To address this global health issue, we studied the potential of Nano-Poly-BA in the management of fructose intake and prevention of the resulting liver steatosis. To study the management of fructose intake, we detected the fructose levels in portal vein of mice after gavage of fructose and with or without P1 nanocomplex (Fig. 5A). P1 nanocomplex lowered the portal vein fructose level in 30 min (Fig. 5B), thus reducing the fructose flux into the liver. We further studied the prophylactic effect of Nano-Poly-BA on fatty liver in an early stage NAFLD mouse model. As the hallmark of NAFLD, hepatic triglyceride (TG) accumulation was obviously increased in fructose group than in water control group, as depicted by the raised TG level (39.7 ± 19.9%) detected in the liver homogenates (Fig. 5C) and validated by the erubescent Oil Red O staining liver section (Fig. 5, D and E). On the other hand, P1 nanocomplex efficiently reduced the TG level in the liver (45.1 ± 21.2% lowered, compared to fructose group) to a similar level with control group (Fig. 5, C, D, and F). Free fatty acid, the major indicator of lipotoxicity in the liver and main contributor to the pathogenesis of NASH (*28*), was elevated after the fructose intake, which was also reduced by Nano-Poly-BA (Fig. 5C). In addition, Nano-Poly-BA reduced the total cholesterol (Fig. 5C). These results collectively suggested that Nano-Poly-BA reduced fructose absorption in GI tract and prevented the resulting hepatic steatosis. Nano-Poly-BA may have notable benefit on the prophylaxis and treatment of NAFLD, NASH, and other fructose related diseases.

DISCUSSION

In summary, the oral Nano-Poly-BA is nonfouling and nonabsorbed in the GI tract. It can effectively bind to a full spectrum of saccharides, therefore controlling multiple disorders of carbohydrate metabolism, such as type 1 diabetes, type 2 diabetes, and NAFLD. More detailed studies on the molecular level chemical interactions between the polymer nanocomplex and saccharides in the GI environment will be one of next steps. When Nano-Poly-BA is chemically optimized for a specific setting to manage a specific metabolic disorder, an elaborate study is needed to elucidate the underlying physiological mechanism. Additional preclinical studies in large animals with more complicated food will provide necessary information to further improve formulations for human studies. Before the clinical development, long-term safety studies in nonrodent species could give us more safety understandings on this gut-restricted polymer drugs.

It is still an unmet need to control PPG for some severe diabetics. For these patients, to suppress the uncontrolled glucose level, using a strong glucose lowering agent, e.g., fast-acting insulin, does not

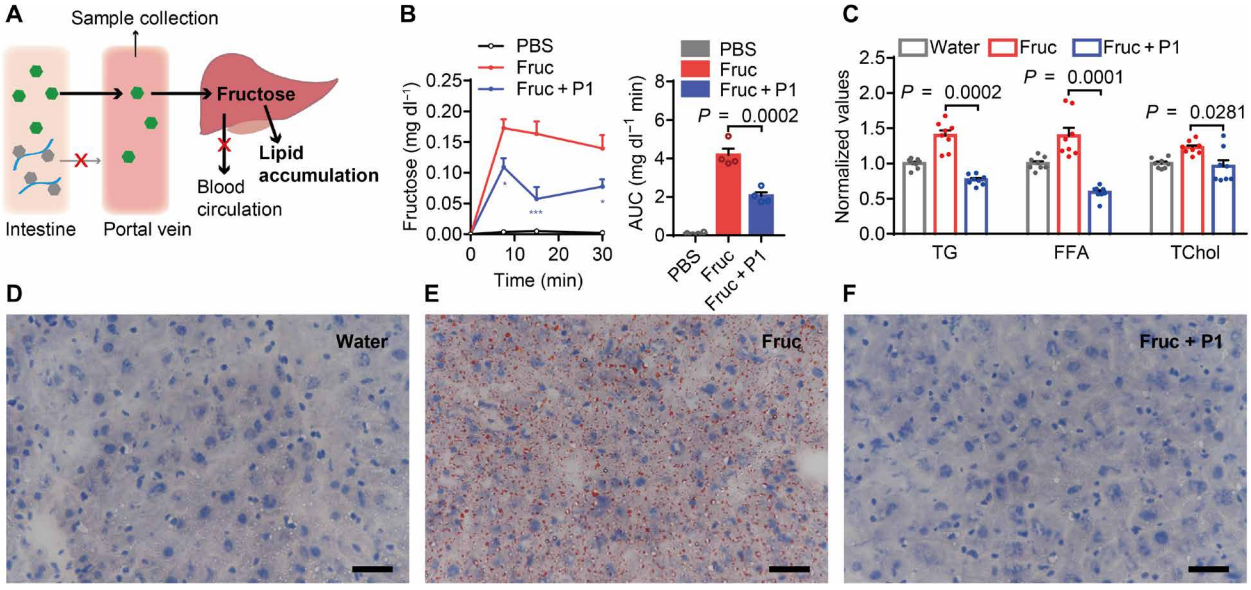

Fig. 5. Control of fructose level for the prevention of liver steatosis. (**A**) Schematic representing that Nano-Poly-BA binds fructose and prevents its absorption in GI tract, which otherwise will be transported through the portal vein into the liver. Distinct from glucose, fructose is mostly metabolized to lipid molecules and accumulated in the liver causing liver diseases; thus, fructose can only be detected in portal vein. (**B**) Relative fructose levels in portal vein and AUC of the curves of mice after oral administration of fructose with or without P1, and control PBS solution, demonstrating P1 greatly reduced GI absorption of fructose. $n = 4$, significant difference analysis between Fruc and Fruc + P1; two-way ANOVA for the curves with $^{*}P \leq 0.05$ and $^{***}P \leq 0.001$, one-way ANOVA for the columns. (**C**) Three groups of mice were set for 1-week free drinking of water, fructose solution, and fructose + P1 solution. One-way ANOVA, $n = 8$. The levels of three lipid biomolecules, triglyceride (TG), free fatty acid (FFA), and total cholesterol (TChol) in liver, and representative images of Oil Red O–stained liver sections of mice given (**D**) water, (**E**) fructose, and (**F**) fructose + P1 indicated a beneficial effect in preventing the liver pimelosis. Scale bars, 50 μm. Error bars show SEM.

always interpret a better treatment efficacy, in the case of lethal hypoglycemia onset and the depressing consequence of weight gain. Acarbose, as an oral drug to lower after-meal blood glucose, lacks these problems and is more patient-friendly than the injectable insulin. Thus, acarbose does occupy a comparatively big diabetic market share in Asia. However, the same popularity does not exist in Western countries, because of its ineffectiveness on monosaccharides (*9*, *10*). Here, Nano-Poly-BA reduces sugar GI intake and covers all sugar types. Nano-Poly-BA may provide a new option for those patients who do not like injection or are vulnerable to hypoglycemia. For patients with impaired renal function, systemic drugs are contraindicated, as they require kidney excretion and increase the burden of already impaired kidney. Nano-Poly-BA, as an oral nonabsorbed drug, will help those patients to control PPG without further renal injury.

MATERIALS AND METHODS

Materials

4-VPBA, acrylic acid (AA), 3-sulfopropyl acrylate potassium salt, 2-(dimethylamino)ethyl acrylate, [2-(acryloyloxy)ethyl]trimethylammonium chloride, PEG methyl ether acrylate [PEGA; weight-average molecular weight (M_w) = 480], 2-hydroxyethyl acrylate, 2-methoxyethyl acrylate, butyl acrylate, fluorescein *o*-acrylate, sodium persulfate ($Na_2S_2O_8$), sodium bisulfite ($NaHSO_3$), tetramethylethylenediamine (TEMED), ammonium persulphate, sodium hydroxide (NaOH), SDS, PEG (average M_w = 400), sodium polyacrylate (PAAS; average M_w = 5000), glucose, fructose, maltose, sucrose, dextrin, starch, hydrochloric acid (37%), sodium bicarbonate, 2-(*N*-morpholino) ethanesulfonic acid, 1-(3-dimethylaminopropyl)-3-ethylcarbodiimide hydrochloride, *N*-hydroxysulfosuccinimide sodium salt, acarbose, STZ, α-glucosidase, amylase, ^{13}C-labeled fructose, deuterium oxide (D_2O), isoflurane, glucose assay kit, cholesterol quantification assay kit, triglyceride quantification colorimetric kit, free fatty acid quantitation kit, and total protein kit were used as received from Sigma-Aldrich. Sulfo-Cy5 amine was purchased from Xi'an Ruixi Biological Technology Co., Ltd. Phosphate buffer (1× PBS, pH 7.4) and sodium citrate buffer (0.1 M, pH 4.5) were purchased from Thermo Fisher Scientific. The 10% SDS–polyacrylamide gel electrophoresis (PAGE) Gel SuperQuick Preparation Kit, prestained color protein marker solution, and SDS-PAGE protein staining and loading buffer were purchased from Beyotime Biotechnology. Optimal cutting temperature (OCT) compound was purchased from Solarbio Life Sciences. One liter of SIF (pH 6.8) was made by dissolving 6.8 g of KH_2PO_4 and 0.896 g of NaOH in water and adjusting to 1000 ml with distilled deionized water (dd-H_2O).

Synthesis of Poly-BA

Poly-BAs were synthesized by the free radical copolymerization of 4-VPBA with different comonomers in aqueous solution by two methods to tune their molecular weights. In method 1, overdose of chain transfer agent was added to obtain polymers with low molecular weight. As an example, P1 was polymerized with 4-VPBA and AA as the comonomers in the mass ratio of 1/1 (molar ratio as 1/2), $NaHSO_3$ as a chain transfer agent in 8 weight % (wt %) of the monomers, and $Na_2S_2O_8$ as an initiator in 1.6 wt % of the monomers. SDS and PEG were added as the surfactants to form the microemulsion. As a general synthesis route, to a solution of 4-VPBA (1480.0 mg, 10.0 mmol), AA (1480.0 mg, 20.6 mmol), $NaHSO_3$ (236.8 mg, 2.3 mmol), PEG (15,780.0 mg, 39.5 mmol), and SDS (3950.0 mg,

13.7 mmol) in 40 ml of dd-H_2O was added a solution of $Na_2S_2O_8$ (47.4 mg, 0.2 mmol) in 2 ml of dd-H_2O dropwise. The reaction was stirred at 72°C overnight for polymerization. The polymer solution was neutralized by 1 M NaOH aqueous solution and then transferred to a circulation system supported by a peristaltic pump in connection with cross flow cassettes [Sartorius Vivaflow 50, molecular weight cut-off (MWCO) = 10,000] for purification and concentration (fig. S1). After lyophilization, P1 was obtained as a white solid with an average yield of 91%. P20 was synthesized in the same process as that of P1 but with different species and ratios of comonomers. Feed ratios (weight, molar) of comonomers for P20: 4-VPBA/AA/PEGA = 1/0.5/0.5 and 1/1/0.15; average yield for the polymerization of P20 was about 85%. As shown in table S1, copolymers P1 to P8 (M1 to M8 in Fig. 2), P13 to P18 (fig. S7), and P19 to P21 (fig. S10) were all synthesized in the same process as that of P1 (method 1) but with different species and ratios of comonomers. 4-VPBA was further copolymerized with comonomers M1, M4, M5, and M7 by method 2, to obtain copolymers P9 to P12 (fig. S5) with relatively high molecular weights. As an example, copolymer P9 was synthesized with following procedure. To a solution of 4-VPBA (1480.0 mg, 10.0 mmol), AA (1480.0 mg, 20.6 mmol), TEMED [3.0 mg, 25.8 μmol, 0.5 mole percent (mol %) of the monomers], PEG (7890.0 mg, 19.8 mmol), and SDS (1975.0 mg, 6.9 mmol) in 40 ml of dd-H_2O was added a solution of ammonium persulphate (11.4 mg, 50.0 μmol, 1 mol % of the monomers) in 2 ml of dd-H_2O dropwise. The reaction was stirred at 45°C overnight for polymerization. The purification and drying process was as same as that of P1. P10 to P12 were synthesized in the same process as that of P9 but with different species of comonomers. Fluorescein-labeled Poly-BAs were synthesized in dark with the same process as the unlabeled counterparts (P1, P4, P5, and P8), but fluorescein *o*-acrylate (1 mol % of 4-VPBA, 0.1 mmol) was added during the polymerization.

In vitro enzymolysis tests of disaccharides and polysaccharides with Poly-BA in SIF

Disaccharides and polysaccharides are digested by enzymes before absorption by intestine epithelium in human body. To examine the efficacy of the polymers to block saccharides from enzymolysis in the intestine lumen, in vitro tests were performed in SIF to simulate the process in vivo. Typically, for disaccharides (maltose or sucrose), 10 ml of polymer solution (0.1 to 10 mg/ml), 10 ml of disaccharide solution (10 mg/ml), and 10 ml of α-glucosidase solution (1.0 mg/ml) were prepared separately using SIF as solvent and were mixed. As a control group, disaccharide was mixed with α-glucosidase without polymer. For polysaccharides, two kinds of enzymes (α-glucosidase and amylase) were added together to degrade polysaccharides (starch, dextrin, or glycogen) down to glucose. Six replicates of mixed solutions for each polymer and saccharide conditions were incubated at 37°C on a shaker plate at 200 rpm for 4 hours. Then, the glucose levels in each solution were measured by glucose oxidase-peroxidase method using a glucose (GO) assay kit (Sigma-Aldrich) and a microplate reader (Infinite M1000 PRO, Tecan). Typically, 10 μl of testing solution was diluted with 950 μl of SIF and then added with 2.0 ml of glucose assay reagent, incubated for 30 min at 37°C, quenched by adding 2.0 ml of 6 M H_2SO_4, and measured the absorbance at 540 nm. The glucose level was calculated by comparing the absorbance of samples with the glucose standard (1 mg/ml). Degree of hydrolysis is defined as the fraction (or percentage) of the total complex saccharides (polysaccharides and disaccharides), which is hydrolyzed. It is calculated by dividing the detected glucose level by the theoretical glucose level of 100% hydrolysis. For example, as for 1 M maltose, its theoretical glucose level after complete hydrolysis should be 2 M; if the detected glucose level is 1.5 M, the degree of hydrolysis equals to 1.5 divided by 2, which is 75%. Statistical significance was determined using one-way analysis of variance (ANOVA) with $^*P \leq 0.05$, $^{**}P \leq 0.01$, $^{***}P \leq 0.001$, and $^{****}P \leq 0.0001$.

Glucose absorption tests using a dialysis method

Glucose is absorbed directly by intestine epithelium. To examine the capacity of the polymers to intercept glucose from absorption, an in vitro simulation tests were carried out. A dialysis bag (MWCO = 1.0 kDa) was prepared as a physical barrier to mimic the intestinal tract spatially with the interior and the exterior space that referred to intestine lumen and the inner system of the body, respectively. Typically, 2.4 g of P1 and 2.4 g of glucose were dissolved in 8 ml of SIF, and then, the solution was transferred into a dialysis bag placed in a 50-ml centrifuge tube. Thirty milliliters of PAAS SIF solution (300 mg/ml) was added to the tube to keep the same polymeric osmotic pressure outside with inside. As a control group, 2.4 g of PAAS polymer was added into the dialysis bag instead of P1. The tubes were kept at 37°C on a shaker plate at 100 rpm, and at each predetermined time point, 10-μl solution outside the dialysis bag was withdrawn and diluted 20 times for the glucose measurement. Areas under the curves (AUCs) were calculated with the initial glucose concentration (0 mg/ml) as the baseline. Statistical significance was determined using two-way ANOVA for the dialysis curves and Student's *t* tests (two tailed) for the AUC results with $^*P \leq 0.05$, $^{**}P \leq 0.01$, $^{***}P \leq 0.001$, and $^{****}P \leq 0.0001$.

Animals

All procedures were conducted in agreement with the guideline of the Institutional Animal Care and Use Committee of Shanghai Jiao Tong University. Male C57BL/6J mice (6 to 8 weeks) were purchased from Shanghai SLAC Laboratory Animal. DIO mice were obtained from Model Animal Research Center of the Nanjing University and were used as type 2 diabetic mouse model. The type 1 diabetic mouse model was induced by STZ injection to C57BL/6J mice. The STZ solution [10 mg/ml in sodium citrate buffer (pH 4.5)] was freshly made and sterilized by filtering with 0.22-μm Millipore filter membrane before use. After fast for 12 hours, each mouse was injected intraperitoneally with 0.2 ml of STZ solution in a dose of 60 mg/kg per day for 5 days consecutively. Fasting plasma glucose of mice was measured 1 week after injection, and mice with fasting glucose levels over 16.7 mM were selected for further study. All mice were acclimatized under a 12-hour light/12-hour dark cycle for at least 1 week with ad libitum access to normal chow or high-fat mouse chow (D12492 from Research Diets Inc. for DIO mice).

One-week acute toxicity study

To evaluate the acute toxicity of the polymer, gavage was carried out on C57BL/6J male mice with Poly-BA (P1 or P20) solution in a dose of 5 g/kg (0.2 ml and 2.5 g/kg for each gavage, twice gavage a day) per day for 7 days. Mice given PBS was regarded as the control group. Mortality, body weight (fig. S15), water and food consumption, and any other adverse effects were monitored carefully. Mice were euthanized and dissected after 7-day gavage. Anatomy observation was focused on GI lesion and bowel obstruction, which were the major concerns for these nonabsorbed medicines.

To assess the potential localized adverse effects of the polymer on GI tract, mice were supplied with P1 aqueous solution (5 wt %) or normal sterilized water for 1 week with body weight, water, and food intake recorded. To avoid the possible harm by frequent gavage, we added P1 into drinking water for free consumption. At the end of the experiment, mice were euthanized, and GI tracts were harvested for histological assessments (Fig. 3K). The histological procedure: The freshly harvested GI tracts were washed gently with cold saline, fixed in 4% paraformaldehyde for 24 hours, dehydrated using graded ethanol, vitrificated by dimethylbenzene, embedded in paraffin, and sectioned with 5-μm thickness. The sections were further stained using hematoxylin and eosin staining.

Mucus retention test of Poly-BAs on porcine duodenum

To identify the contributions of different comonomers to the nofouling fouling nature of Poly-BAs on intestinal mucus, we conducted an ex vivo mucus retention test. The proximal duodenums of five male (castrated) finishing pigs (Duroc × Landrace × Large White, weighing 110 to 130 kg) were collected from a local abattoir. A 6- to 8-cm section of fresh porcine duodenum was isolated, opened, and gently washed. Fluorescein-labeled Poly-BAs [shown as M1, M4, M5, and M8 in Fig. 2 (D and E)] were synthesized by adding fluorescein *o*-acrylate (1 mol % of monomers) into the copolymerization of 4-VPBA with M1/M4/M5/M8. Fluorescein-labeled Poly-BA solution (150 μl, 10 mg/ml) was dropped onto the internal surface (mucosa) of duodenum. Ten minutes later, the duodenum was washed with 1 ml of PBS. Images were captured by a small-animal imaging system [Caliper In Vivo Imaging System (IVIS) Lumina II]. The polymer retention on mucus was revealed by the fluorescence retention, calculated from the fluorescent intensity results of the images by (after washing − original)/(after adding − original).

Hydrodynamic size measurement of P1

Nano-Poly-BA aggregates into nanocomplex in water by the supramolecular interaction (hydrogen bond) between boronic acid groups and carboxylic acid groups. The dense distribution of boronic acid groups and carboxylic acid groups has large capability to encapsulate and trap the saccharide molecules by both dynamic covalent bonds and hydrogen bonds. By swelling and binding of saccharides, Nano-Poly-BA is supposed to be inflated. DLS measurement was carried out in NanoBrook 90Plus particle size analyzer to monitor the dimensional change of Nano-Poly-BA in SIF to demonstrate the binding of saccharide onto Nano-Poly-BA. P1 (2 mg/ml), sucrose (2 mg/ml), and maltose (2 mg/ml) in SIF were prepared and filtered with 0.45-μm membrane. P1 solution was mixed with SIF, sucrose, or maltose solution 1/1 (v/v) to obtain samples as *P1*, *P1 + Suc*, and *P1 + Mal*, which were incubated for 5 min before testing. Scattering light was detected at 90°.

Fluorescence imaging of mouse body and selected organs with polymer gavage

Near-infrared dye-labeled (sulfo-Cy5) P1 was used to study the biodistribution and elimination in mouse model. Mice were either kept fasting until the end of the test (Fig. 3) or set for free access to standard chow (fig. S16) to exclude or incorporate the impact of uncontrolled food intake. The IVIS Lumina III In Vivo Imaging System was used for mouse fluorescence imaging. For in vivo imaging, mice were orally administered with sulfo-Cy5–labeled polymer (0.2 ml, 1.0 g/kg, or 125 mg/ml for mouse body weight of 25 g) at $t = 0$ min and were sedated with isoflurane at each time point. Images were captured with excitation at 650 nm and emission at 670 nm. Imaging reconstructing and analysis were accomplished through Living Image Software. For ex vivo imaging, mice were euthanized at each time point and dissected immediately; GI tract and selected viscera were fetched and arranged on clean dishes for imaging.

Table 1. The carbohydrate composition and contents of real-world carbohydrate-containing foods and drinks used in Fig. 4 (H to J), which were obtained on the basis of original commodity information or roughly estimated (for porridge). HFCS, high-fructose corn syrup.

	Blueberry jam	Coke	Porridge
Species	HFCS, sucrose	HFCS, sucrose	Starch
Contents/wt %	62.5	10.6	10.0

Table 2. The dosages of real-world carbohydrate-containing foods and drinks used in Fig. 4 (H to J).

	Blueberry jam	Coke	Porridge	P1
Lean mice	0.2 ml	0.4 ml	0.2 ml	1.5 g/kg, 0.2 ml
DIO mice	0.05 ml + 0.15 ml dd-H_2O	0.2 ml	0.05 ml + 0.15 ml dd-H_2O	1 g/kg, 0.2 ml

OGTT, OCTT, and IPGTTs

OGTT and OCTT (Fig. 4, A to G) were the main method to evaluate the efficacy of boric polymers on cutting down mealtime carbohydrate absorption, and IPGTT (fig. S17) were carried out to testify the nonsystematic effect of P1 on lowering glucose. As a standard OGTT or OCTT procedure, mice were fasted overnight, generally 13 hours starting from 8 p.m. the day before the test to the next 9 a.m. before a fasting glucose measurement ($t = 0$ min), and gavaged with 0.2 ml of polymer (wild-type mice, 0.2 to 1.5 g/kg; DIO mice/STZ mice, 1.0 g/kg), acarbose (10 mg/kg), or PBS solution 15 min before gavage of 0.2 ml of carbohydrate solution (glucose, maltose, sucrose, or dextrin) in the predetermined dose (2.0 g/kg for wild-type mice, 0.5 g/kg for DIO mice, and 1.0 g/kg for STZ mice). Different mouse models showed different glycemic responses even with the same saccharide and the same dose. The different doses of saccharides for different mouse models were determined to get similar glycemic response (glycemic excursion of 100 to 200 mg dl^{-1}) and to limit the peak glucose level below the detection threshold of the glucometer (600 mg dl^{-1}). All the compounds and carbohydrates were dissolved in PBS with concentration calculated on the basis of body weights for each mouse, and the volume for each gavage was fixed on 0.2 ml. Plasma glucose levels were measured with a drop of blood collected from tail vein using a glucometer (Accu-Chek, Roche) at 15, 30, 60, 90, and 120 min (and 180 min for DIO and STZ mice) after last gavage ($n = 8$ per arm for wild-type and STZ mice and $n = 7$ per arm for DIO mice). Time interval was controlled for each mouse. Data points of glucose level were plotted with time. GE was defined as the difference of glucose level between the peak value and the initial value at $t = 0$ min. iAUC of the tests on wild-type

and DIO mice and pAUC of the tests on STZ mice were calculated on the basis of the plot with the glucose level before gavage as a baseline. *P* values of glucose curves were determined by two-way ANOVA and that of iAUC and pAUC results by one-way ANOVA with $*P \leq 0.05$, $**P \leq 0.01$, $***P \leq 0.001$, and $****P \leq 0.0001$. In IPGTT tests, mice were treated the same as in the OGTT tests except that the glucose solution was injected into the peritoneum instead of gavage, to measure the changes in the glucose level for 2 hours ($n = 8$ per arm).

Real-world food challenge tests

To evaluate the performance of P1 on real food, we challenged both lean mice (C57BL/6J, male) and obese mice (DIO mice, male) with high-carb foods in real life (Fig. 4, H to J) instead of refined carbohydrates (Fig. 4, A to G). Blueberry jam, coke, and porridge were used because of their high popularity. Blueberry jam and coke were purchased from supermarket, and plain porridge was homemade from Chinese rice. All these foods were homogenized before tests so as to be easy to gavage. The carbohydrate composition and contents of these carbos were obtained on the basis of original commodity information or roughly estimated (for porridge) and were listed in Table 1. The dosages of carbos were presented in Table 2. The dosage used in DIO mice group were lowered to ensure that the glucose levels measured would not exceed the detection range of glucometer. *P* values were calculated by one-way ANOVA with $*P \leq 0.05$, $**P \leq 0.01$, $***P \leq 0.001$, and $****P \leq 0.0001$.

Oral fructose challenge tests

To determine the efficacy of Poly-BA on reducing fructose absorption, we conducted an oral fructose challenge test. Ingested fructose was transported through portal vein into liver, then was fast-metabolized in liver, and seldom exists in blood circulation (Fig. 5A). Therefore, we detected the fructose levels in portal vein of mice (C57BL/6), after gavage of fructose (1.0 g/kg) with or without P1 (1.5 g/kg) or PBS. Blood samples were collected using a reported method (*29*). Typically, mice were anesthetized with isoflurane via a nose cone. Then, the abdominal cavity was opened, and intestines were displaced to identity the portal vein. We used a springe to extract portal vein blood (~100 μl) different time after gavage (7.5, 15, and 30 min). The blood samples were placed on ice in the absence of anticoagulant for 25 min, centrifuged at 12,000*g* for 10 min at 4°C to be made into serum, and extracted by methanol:acetonitrile:water (40:40:20). The extracts were analyzed by liquid chromatography–mass spectrometer with ^{13}C-labeled fructose as the internal label. $n = 4$, two-way ANOVA for the fructose curves with $*P \leq 0.05$, $**P \leq 0.01$, $***P \leq 0.001$, and $****P \leq 0.0001$, one-way ANOVA for the AUC results.

Early-stage fatty liver model induced by fructose

Fructose was metabolized in liver majorly to generate lipid that could be pathogenic when overloading. A fructose-induced early-stage fatty liver model was used to evaluate the potential benefit of P1 on fatty liver-based diseases. Mice were divided into three groups, placebo group with free drinking normal water, fructose group with fructose solution (20 wt %), and P1 group with mixed solution of fructose (20 wt %) and P1 (5 wt %), lasting for 15 days. Mice were euthanized, and the livers were isolated for biochemical and histological analysis. For biochemistry detection, livers were quickly dissected, frozen in liquid nitrogen, and ground with a Cryomill (KH-III-F, Servicebio). The ground tissues were extracted with nine equivalents of cold normal saline at 4°C for 4 hours, followed by vortexing and centrifugation at 4000*g* for 10 min. The supernatant was put to the biochemical assay kits for measurement of total cholesterol, TG, and free fatty acid, respectively, and also for measurement of total protein content. The normalized levels of total cholesterol, TG, and free fatty acid were calculated by dividing the detected levels by the total protein content of each sample. For histological analysis, the freshly harvested liver tissues were washed with cold saline, embedded in OCT compound, and frozen-sectioned with 5-μm thickness. The sections were further stained with Oil Red O and hematoxylin for the evaluation of TG level. *P* values were calculated by one-way ANOVA with $*P \leq 0.05$, $**P \leq 0.01$, $***P \leq 0.001$, and $****P \leq 0.0001$. For histological analysis, livers were frozen-sectioned and stained by Oil Red O to visualize the TG accumulation. Sections were observed under a Nikon NI-E upright microscope.

SUPPLEMENTARY MATERIALS

Supplementary material for this article is available at http://advances.sciencemag.org/cgi/content/full/7/14/eabf7311/DC1

REFERENCES AND NOTES

1. World Health Organization, *The Double Burden of Malnutrition: Policy Brief* (World Health Organization, 2016).
2. S. S. Lim, T. Vos, A. D. Flaxman, G. Danaei, K. Shibuya, H. Adair-Rohani, M. Amann, H. R. Anderson, K. G. Andrews, M. Aryee, C. Atkinson, L. J. Bacchus, A. N. Bahalim, K. Balakrishnan, J. Balmes, S. Barker-Collo, A. Baxter, M. L. Bell, J. D. Blore, F. Blyth, C. Bonner, G. Borges, R. Bourne, M. Boussinesq, M. Brauer, P. Brooks, N. G. Bruce, B. Brunekreef, C. Bryan-Hancock, C. Bucello, R. Buchbinder, F. Bull, R. T. Burnett, T. E. Byers, B. Calabria, J. Carapetis, E. Carnahan, Z. Chafe, F. Charlson, H. Chen, J. S. Chen, A. T. Cheng, J. C. Child, A. Cohen, K. E. Colson, B. C. Cowie, S. Darby, S. Darling, A. Davis, L. Degenhardt, F. Dentener, D. C. Des Jarlais, K. Devries, M. Dherani, E. L. Ding, E. R. Dorsey, T. Driscoll, K. Edmond, S. E. Ali, R. E. Engell, P. J. Erwin, S. Fahimi, G. Falder, F. Farzadfar, A. Ferrari, M. M. Finucane, S. Flaxman, F. G. Fowkes, G. Freedman, M. K. Freeman, E. Gakidou, S. Ghosh, E. Giovannucci, G. Gmel, K. Graham, R. Grainger, B. Grant, D. Gunnell, H. R. Gutierrez, W. Hall, H. W. Hoek, A. Hogan, H. D. Hosgood, D. Hoy, H. Hu, B. J. Hubbell, S. J. Hutchings, S. E. Ibeanusi, G. L. Jacklyn, R. Jasrasaria, J. B. Jonas, H. Kan, J. A. Kanis, N. Kassebaum, N. Kawakami, Y. H. Khang, S. Khatibzadeh, J. P. Khoo, C. Kok, F. Laden, R. Lalloo, Q. Lan, T. Lathlean, J. L. Leasher, J. Leigh, Y. Li, J. K. Lin, S. E. Lipshultz, S. London, R. Lozano, Y. Lu, J. Mak, R. Malekzadeh, L. Mallinger, W. Marcenes, L. March, R. Marks, R. Martin, P. McGale, J. McGrath, S. Mehta, G. A. Mensah, T. R. Merriman, R. Micha, C. Michaud, V. Mishra, K. M. Hanafiah, A. A. Mokdad, L. Morawska, D. Mozaffarian, T. Murphy, M. Naghavi, B. Neal, P. K. Nelson, J. M. Nolla, R. Norman, C. Olives, S. B. Omer, J. Orchard, R. Osborne, B. Ostro, A. Page, K. D. Pandey, C. D. Parry, E. Passmore, J. Patra, N. Pearce, P. M. Pelizzari, M. Petzold, M. R. Phillips, D. Pope, C. A. Pope, J. Powles, M. Rao, H. Razavi, E. A. Rehfuess, J. T. Rehm, B. Ritz, F. P. Rivara, T. Roberts, C. Robinson, J. A. Rodriguez-Portales, I. Romieu, R. Room, L. C. Rosenfeld, A. Roy, L. Rushton, J. A. Salomon, U. Sampson, L. Sanchez-Riera, E. Sanman, A. Sapkota, S. Seedat, P. Shi, K. Shield, R. Shivakoti, G. M. Singh, D. A. Sleet, E. Smith, K. R. Smith, N. J. Stapelberg, K. Steenland, H. Stöckl, L. J. Stovner, K. Straif, L. Straney, G. D. Thurston, J. H. Tran, R. Van Dingenen, A. van Donkelaar, J. L. Veerman, L. Vijayakumar, R. Weintraub, M. M. Weissman, R. A. White, H. Whiteford, S. T. Wiersma, J. D. Wilkinson, H. C. Williams, W. Williams, N. Wilson, A. D. Woolf, P. Yip, J. M. Zielinski, A. D. Lopez, C. J. Murray, M. Ezzati, M. A. AlMazroa, Z. A. Memish, A comparative risk assessment of burden of disease and injury attributable to 67 risk factors and risk factor clusters in 21 regions, 1990–2010: A systematic analysis for the Global Burden of Disease Study 2010. *Lancet* **380**, 2224–2260 (2012).
3. M. B. Vos, J. L. Kaar, J. A. Welsh, L. V. Van Horn, D. I. Feig, C. A. M. Anderson, M. J. Patel, J. C. Munos, N. F. Krebs, S. A. Xanthakos, R. K. Johnson; American Heart Association Nutrition Committee of the Council on Lifestyle and Cardiometabolic Health; Council on Clinical Cardiology; Council on Cardiovascular Disease in the Young; Council on Cardiovascular and Stroke Nursing; Council on Epidemiology and Prevention; Council on Functional Genomics and Translational Biology; and Council on Hypertension, Added sugars and cardiovascular disease risk in children: A scientific statement from the American Heart Association. *Circulation* **135**, e1017–e1034 (2017).
4. V. S. Malik, B. M. Popkin, G. A. Bray, J.-P. Després, W. C. Willett, F. B. Hu, Sugar-sweetened beverages and risk of metabolic syndrome and type 2 diabetes: A meta-analysis. *Diabetes Care* **33**, 2477–2483 (2010).

5. D. S. Ludwig, K. E. Peterson, S. L. Gortmaker, Relation between consumption of sugar-sweetened drinks and childhood obesity: A prospective, observational analysis. *Lancet* **357**, 505–508 (2001).
6. T. Jensen, M. F. Abdelmalek, S. Sullivan, K. J. Nadeau, M. Green, C. Roncal, T. Nakagawa, M. Kuwabara, Y. Sato, D. H. Kang, D. R. Tolan, L. G. Sanchez-Lozada, H. R. Rosen, M. A. Lanaspa, A. M. Diehl, R. J. Johnson, Fructose and sugar: A major mediator of non-alcoholic fatty liver disease. *J. Hepatol.* **68**, 1063–1075 (2018).
7. R. J. Johnson, M. S. Segal, Y. Sautin, T. Nakagawa, D. I. Feig, D.-H. Kang, M. S. Gersch, S. Benner, L. G. Sánchez-Lozada, Benner, Potential role of sugar (fructose) in the epidemic of hypertension, obesity and the metabolic syndrome, diabetes, kidney disease, and cardiovascular disease. *Am. J. Clin. Nutr.* **86**, 899–906 (2007).
8. B. M. Popkin, C. Hawkes, Sweetening of the global diet, particularly beverages: Patterns, trends, and policy responses. *Lancet Diabetes Endocrinol.* **4**, 174–186 (2016).
9. H. E. Lebovitz, Alpha-glucosidase inhibitors. *Endocrinol. Metab. Clin. North Am.* **26**, 539–551 (1997).
10. Q. Zhu, Y. Tong, T. Wu, J. Li, N. Tong, Comparison of the hypoglycemic effect of acarbose monotherapy in patients with type 2 diabetes mellitus consuming an Eastern or Western diet: A systematic meta-analysis. *Clin. Ther.* **35**, 880–899 (2013).
11. A. Abramson, E. Caffarel-Salvador, M. Khang, D. Dellal, D. Silverstein, Y. Gao, M. R. Frederiksen, A. Vegge, F. Hubalek, J. J. Water, A. V. Friderichsen, J. Fels, R. K. Kirk, C. Cleveland, J. Collins, S. Tamang, A. Hayward, T. Landh, S. T. Buckley, N. Roxhed, U. Rahbek, R. Langer, G. Traverso, An ingestible self-orienting system for oral delivery of macromolecules. *Science* **363**, 611–615 (2019).
12. Y. Lee, T. E. Deelman, K. Chen, D. S. Y. Lin, A. Tavakkoli, J. M. Karp, Therapeutic luminal coating of the intestine. *Nat. Mater.* **17**, 834–842 (2018).
13. G. M. Gray, Carbohydrate digestion and absorption—Role of the small intestine. *N. Engl. J. Med.* **292**, 1225–1230 (1975).
14. G. Springsteen, B. Wang, A detailed examination of boronic acid–diol complexation. *Tetrahedron* **58**, 5291–5300 (2002).
15. J. Wang, J. Yu, Y. Zhang, X. Zhang, A. R. Kahkoska, G. Chen, Z. Wang, W. Sun, L. Cai, Z. Chen, C. Qian, Q. Shen, A. Khademhosseini, J. B. Buse, Z. Gu, Charge-switchable polymeric complex for glucose-responsive insulin delivery in mice and pigs. *Sci. Adv.* **5**, eaaw4357 (2019).
16. V. Yesilyurt, M. J. Webber, E. A. Appel, C. Godwin, R. Langer, D. G. Anderson, Injectable self-healing glucose-responsive hydrogels with pH-regulated mechanical properties. *Adv. Mater.* **28**, 86–91 (2016).
17. W. L. Brooks, B. S. Sumerlin, synthesis and applications of boronic acid-containing polymers: From materials to medicine. *Chem. Rev.* **116**, 1375–1397 (2016).
18. S. D. Bull, M. G. Davidson, J. M. H. van den Elsen, J. S. Fossey, A. T. A. Jenkins, Y.-B. Jiang, Y. Kubo, F. Marken, K. Sakurai, J. Zhao, T. D. James, Exploiting the reversible covalent bonding of boronic acids: Recognition, sensing, and assembly. *Acc. Chem. Res.* **46**, 312–326 (2012).
19. R. Ma, L. Shi, Phenylboronic acid-based glucose-responsive polymeric nanoparticles: Synthesis and applications in drug delivery. *Polym. Chem.* **5**, 1503–1518 (2014).
20. E. F. Connor, I. Lees, D. Maclean, Polymers as drugs—Advances in therapeutic applications of polymer binding agents. *J. Polym. Sci. A Polym. Chem.* **55**, 3146–3157 (2017).
21. J. A. DiPalma, P. H. DeRidder, R. C. Orlando, B. E. Kolts, M. B. Cleveland, A randomized, placebo-controlled, multicenter study of the safety and efficacy of a new polyethylene glycol laxative. *Am. J. Gastroenterol.* **95**, 446–450 (2000).
22. M. H. Davidson, M. A. Dillon, B. Gordon, P. Jones, J. Samuels, S. Weiss, J. Isaacsohn, P. Toth, S. K. Burke, Colesevelam hydrochloride (Cholestagel). *Arch. Intern. Med.* **159**, 1893–1900 (1999).
23. M. R. Weir, G. L. Bakris, D. A. Bushinsky, M. R. Mayo, D. Garza, Y. Stasiv, J. Wittes, H. Christ-Schmidt, L. Berman, B. Pitt; OPAL-HK Investigators, Patiromer in patients with kidney disease and hyperkalemia receiving RAAS inhibitors. *N. Engl. J. Med.* **372**, 211–221 (2015).
24. D. A. Bushinsky, T. Hostetter, G. Klaerner, Y. Stasiv, C. Lockey, S. McNulty, A. Lee, D. Parsell, V. Mathur, E. Li, J. Buysse, R. Alpern, Randomized, controlled trial of TRC101 to increase serum bicarbonate in patients with CKD. *Clin. J. Am. Soc. Nephrol.* **13**, 26–35 (2018).
25. Y. Xiao, Y. Hu, J. Du, Controlling blood sugar levels with a glycopolymersome. *Mater. Horiz.* **6**, 2047–2055 (2019).
26. S. K. Lai, Y.-Y. Wang, J. Hanes, Mucus-penetrating nanoparticles for drug and gene delivery to mucosal tissues. *Adv. Drug Deliv. Rev.* **61**, 158–171 (2009).
27. M. Kleinert, C. Clemmensen, S. M. Hofmann, M. C. Moore, S. Renner, S. C. Woods, P. Huypens, J. Beckers, M. H. de Angelis, A. Schürmann, M. Bakhti, M. Klingenspor, M. Heiman, A. D. Cherrington, M. Ristow, H. Lickert, E. Wolf, P. J. Havel, T. D. Müller, M. H. Tschöp, Animal models of obesity and diabetes mellitus. *Nat. Rev. Endocrinol.* **14**, 140–162 (2018).
28. B. A. Neuschwander-Tetri, Hepatic lipotoxicity and the pathogenesis of nonalcoholic steatohepatitis: The central role of nontriglyceride fatty acid metabolites. *Hepatology* **52**, 774–788 (2010).
29. C. Jang, S. Hui, W. Lu, A. J. Cowan, R. J. Morscher, G. Lee, W. Liu, G. J. Tesz, M. J. Birnbaum, J. D. Rabinowitz, The small intestine converts dietary fructose into glucose and organic acids. *Cell Metab.* **27**, 351–361.e3 (2018).
30. D. Roy, J. N. Cambre, B. S. Sumerlin, Sugar-responsive block copolymers by direct RAFT polymerization of unprotected boronic acid monomers. *Chem. Commun.*, 2477–2479 (2008).

Acknowledgments: We are indebted to S. Zhang, C. Zhang, J. Cheng, and J. Liu for fruitful discussions. **Funding:** This work was, in part, supported by the Youth Thousand Talents Program of China, start-up grants from the Shanghai Jiao Tong University (WF220408211). This work was also supported by the grants from the State Key Laboratory of Oncogenes and Related Genes (90-17-02) and from the Interdisciplinary Program of Shanghai Jiao Tong University (YG2017MS18). **Author contributions**: X.Z. and S.Z. designed the material and experiments. J.L., H.Z., and X.Z. synthesized the material. X.Z., H.Z., J.L., M.T., J.Y., S.S., Q.H., L.Y., and S.Z. characterized the material, analyzed the data, and wrote the paper. S.Z. supervised the research. All authors discussed the progress of research and reviewed the manuscript. **Competing interests:** S.Z., X.Z., M.T., S.S., and H.Z. are inventors on a Chinese patent application related to this work filed by the Shanghai Jiao Tong University (no. 201910492851.5, filed on 11 June 2019). The authors declare that they have no other competing interests. **Data and materials availability:** All data needed to evaluate the conclusions in the paper are present in the paper and/or the Supplementary Materials. Additional data related to this paper may be requested from the authors.

Submitted 16 November 2020
Accepted 11 February 2021
Published 31 March 2021
10.1126/sciadv.abf7311

Citation: X. Zhao, H. Zhang, J. Li, M. Tian, J. Yang, S. Sun, Q. Hu, L. Yang, S. Zhang, Orally administered saccharide-sequestering nanocomplex to manage carbohydrate metabolism disorders. *Sci. Adv.* **7**, eabf7311 (2021).